June 9,1998 *CLNS 98/1562*

A Laser Linear Collider Design[1]

A. A. Mikhailichenko[2]
Wilson Laboratory, Cornell University, Ithaca, NY 14853-8001

Abstract. A conceptual design of crucial elements of 2×1 *km* long linac considered. This linac is driven by a laser radiation distributed within open accelerating structures with special sweeping devices. These devices deflect the laser radiation to the structures in accordance with instant position of accelerated particles. The power reduction and shortening the illumination time for every point on the structure equates to the number of resolved spots, associated with this sweeping device. A 300 *J* total, 100-*ps* laser flash could provide the final energy 30 *TeV* for $l\cong 1mm$ and 3 *TeV* for $l\cong 10mm$ on 1 *km* with the method described. This total power required could be generated with amplifiers distributed along the linac. For repetition rate 160 *Hz* the luminosity associated with colliding beams could reach $L\approx 10^{33}cm^{-2}s^{-1}$ per bunch with population 10^7. Wall plug power required for operation of LLC is ~ *2 MW*.

1. INTRODUCTION

The concept of a Linac, driven by a Traveling Laser Focus (TLF) method described in [1]. TLF deals with accelerating structure, what scaled down to a laser wavelength. Each cell of the structure has an opening from one side (so called open acceleration structure). Laser radiation focused onto these openings. This spot of focused radiation has an instant size much smaller, than longitudinal dimension of the structure, thereby exciting the cells of the structure locally. Special sweeping (deflecting) device moves this focal spot in *longitudinal* direction so, that this spot is following the particle in its motion along the accelerating structure. Due to this arrangement, all impulse laser power is acting for generation of accelerating field at the instant particle's location only. By this way total power, required from the laser becomes reduced. The illuminating time for any point on the grating is lowered also. It was shown [1], that the power reduction and shortening of illuminating time is equal numerically to the *number of resolved spots (pixels)*, associated with the sweeping device. The number of resolved spots shows how many times focused laser spot could be positioned along the structure so the length of the structure is covered in full. On the basis of TLF method the scheme for Laser Linear Collider (LLC) was proposed, Fig. 1, [1c]. This general scheme contains many elements, playing an important role in acceleration process. They are the laser sweeping device itself, accelerating structure, focusing elements, injector and the final focusing elements. In this publication we continue consideration of these elements of the LLC. Parameters of this LLC are represented in a Table 1. These parameters reflect two options for the laser wavelength choice. LLC may have *two stages* with two wavelengths also. As far as total laser flash energy (300 *J* in the Table 1), it could be generated either by a single amplifier unit or by *many amplifiers* distributed along the Linac (see Fig. 10 lower). All the linac length is sectioned by modules having the length L~3 *cm*. Within each of these sections the laser

---

[1] *A Talk on 8th Workshop on Advanced Accelerator Concepts, Renaissance Harborplace Hotel, Baltimore, Maryland, July 5-11, 1998, supported by National Science Foundation.*

[2] Phone: (607) 255-3785, Fax: (607) 255-8062, e-mail "mikhail@lns62.lns.cornell.edu

flash having duration $t \cong 100$ *ps* becomes distributed along the length of accelerating structure. Energy required for excitation the field in the structure up to 3*GeV/m* is about 10 *mJ* for the laser wavelength $l \cong 10mm$. For $l \cong 1mm$ this pulse will give 30*GeV/m*. Interaction of beams at IP is going in deep quantum regime. The beams of electrons and positrons can be polarized what gives the effective gain in luminosity and reduces the background [1c,21].

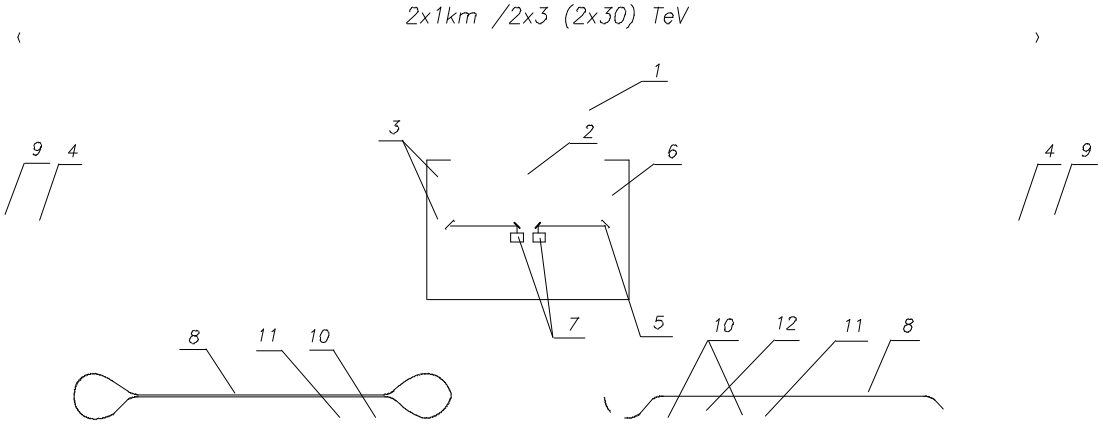

laser impulse power, required for excitation the structure to this level[3]. This method also cuts down the illumination time for every point of the structure. The last brings hope that the break down limit will be increased due to shortening of illuminating pulse duration.

2. TLF METHOD

Fig. 2 reminds the idea [1]. The pulse of laser radiation lasts for a time t, so it has the length $\approx ct$, pos. 1. The laser bunch 1 passed trough splitting devices 7 generated the secondary bunches 2-4. Beam of particles 5 is going inside this structure with velocity *V*. The laser bunch instant positions are numbered by 1-4. Structure 6 has a length *L* in longitudinal direction. Device 9 is electrically driven by electrical pulse for *sweeping* the laser beam in longitudinal direction synchronously with the particle's passage. While arriving to the structure, the laser bunch has a slope a. Angle $Q \cong L/R$, $W \cong c/R$. These parameters connected as

$$Q \cdot \tan a = cL/VR \cong W\,ct/V \cong W \cdot ct/V \cong cQ/V . \qquad (1)$$

For $V \cong c$ this gives evidently $a \cong 45^{o}$. All deflecting elements are synchronized so that the bunch 5 has continuous acceleration in all sections.

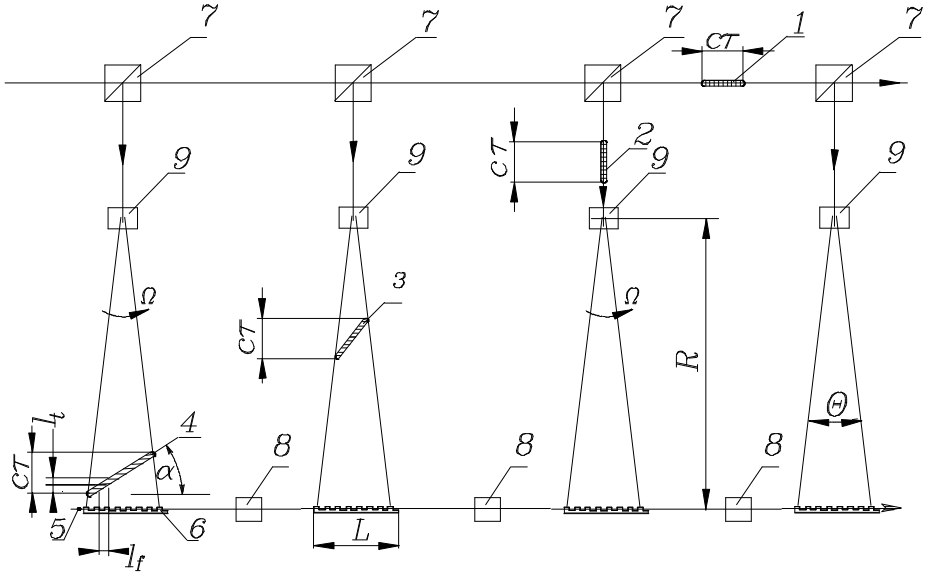

FIGURE 2. Accelerating complex scheme. 1–4–are instant laser beam positions; 1–is a primary laser bunch which is moving from the left side on the picture to the right. 5– is the beam of accelerated particles. 6–is the accelerating structure. 7–are the optical splitters. 8–are the particles' beam focusing elements (if no RF focusing in use). 9–are the deflecting devices.

The laser focus sweep is limited to the distance about 3*cm* for practical reasons (see lower), so the accelerating device looks like a sequence of 3 *cm* long accelerating structures with the focusing elements between them. Filling coefficient could be made about one as the focusing is going through the phase shift in accelerating structures.

A shot focusing *cylindrical* lenses installed on the laser way close to accelerating structure reduce *the transverse size* of the spot to a minimal one pos. 13 in Fig.3. A natural way to increase the deflecting length *R* is utilization of mirrors. Mirrors might be

[3] See Appendix 1.

slightly curved to obtain some focusing properties. Each part of the grating structure is illuminated by duration, which is defined by l_t / c, Fig.2. For example, if we consider $l_t \cong L / N_R \cong 100\, l$, ($N_R$–is the number of resolved spots, see lower), $l = 1mm$, then $l_t / c \cong 3 \cdot 10^{-13} sec$. This time is less than the time between electron-electron collisions $t \approx l_{free} / v_F \cong 10^{-12}\, sec$, where l_{free} – is the free path length, v_F is the electron velocity at Fermi surface [15]. The time of illumination is, however longer, than the time, corresponding to reaction of electron plasma in a metal, what is $t \cong 2p / w_p = 2p / \sqrt{4p n r_0 c^2} \approx 3 \cdot 10^{-16}$ *sec*, where *n*– is the density of electrons, r_0 – is the classical electron radius.

3. GENERAL DESCRIPTION OF LLC

Scaled view of regular part from Fig. 1 is represented in Fig.3 below. To avoid the influence of fluctuations, it was suggested that both beams, the laser–1 and particle's–5 go first to the end of all linear system apart from central station. On this way the bunch's parameters (optical and particle's) picked up and processed with appropriate algorithms. After the bend in systems 2,6 on the *back way to IP* necessary voltages applied to correcting elements, distributed along the linac.

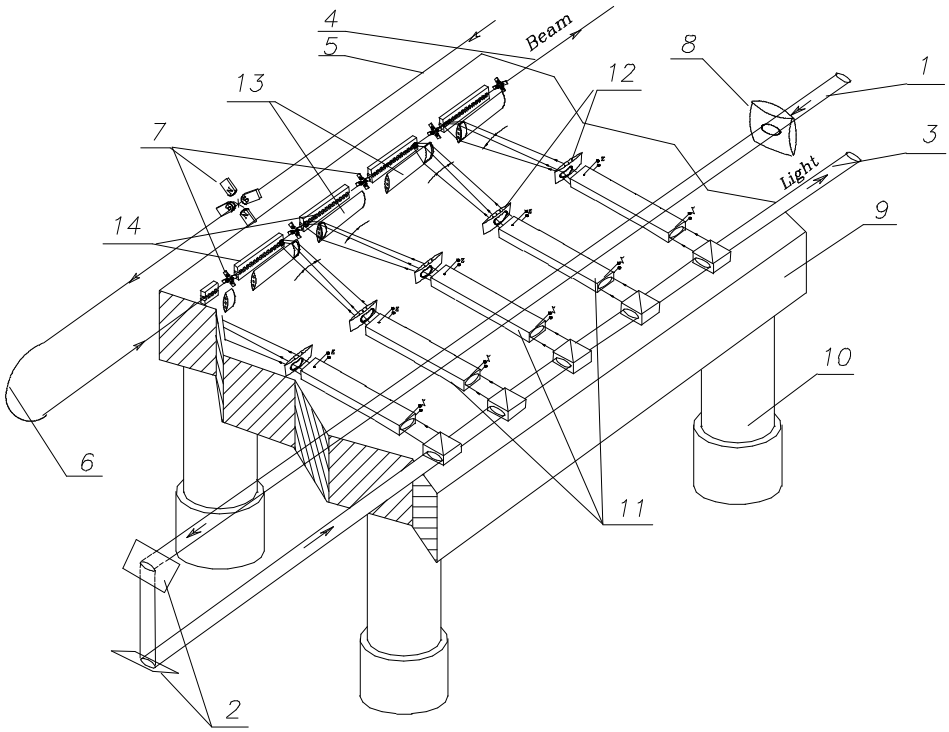

FIGURE 3. Table with a section of accelerator. Comments are in the text.

The particle's beam goes further trough structures to next modules, 4. 7 and 8–are the focusing elements for the particle's and laser beam correspondingly. Optical platform 9 is standing on legs 10 with active damping system to minimize vibrations. Deflecting devices 11 sweep the laser radiation along the accelerating structures 14. 12–are the

lenses for focusing the laser radiation in longitudinal direction. 13–are the short focusing cylindrical lenses.

Example of location of LLC in a tunnel is represented in Fig. 4. The tunnel diameter shown is 3 m. For energy around $0.5 \times 0.5\ GeV$ the LLC could be preferably located on the surface, so any other shape is acceptable.

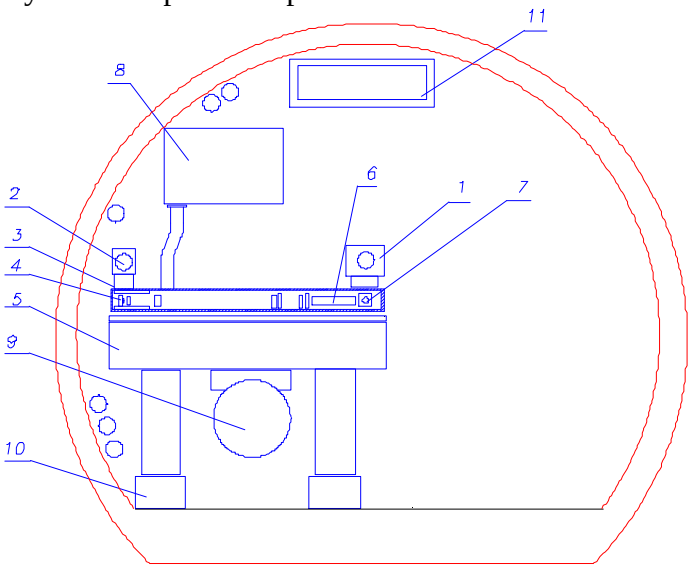

FIGURE 4. Cross section of a tunnel with accelerating system for underground location. 1– is a primary optical beam line. 2–is a primary particle's beam line. 3–is a vacuumed container with all equipment. 4–is an accelerating structure with sub systems. 5–is an optical table. 6–is the deflecting device, 7 –is the line for driving optical beam, 8–is a box with equipment for deflecting device and control. 9–is a tube with optical elements for active alignment of all optical tables. 10–is an anti-vibration active system. 11–is a duct for air conditioning.

4. ACCELERATING STRUCTURE

There are proposals for accelerating structures what could be scaled to match the wavelength of laser radiation [11-13]. We took the foxhole-type structure described in [12] as a basis, Fig. 5. This structure has an advantage in pumping possibilities. The mostly important feature, however, is that this structure gives a good positioning for electrical field map [1c]. Covers 1 adjust the coupling between the groove and outer space. With these covers the height h is about $h \cong l_W / 2$ and the cells have *inductive* coupling with outer space. Structure developed in [13] is close to this type. In original foxhole structure [12] $h \cong 3 l_W / 4$, where

piezoelectric. This allows to align the structures for minimization the wakes. Structures are cooled down to keep the mechanical tolerances within the margins allowed.

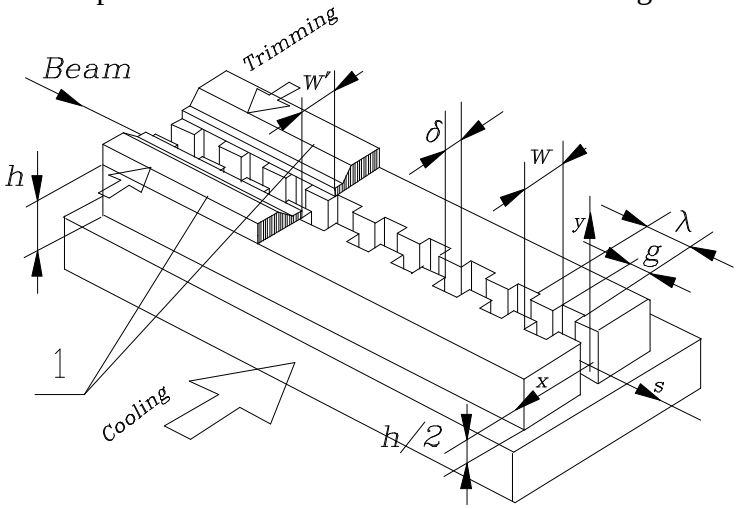

FIGURE 5. The foxhole type accelerating structure. Height h is $h \cong l_W/2$, where l_W –is a wavelength of laser radiation inside the cell. $g/l \cong 1/2$, $W \cong 0.7\,l$, $d \cong 0.2\,l$. 1–are the masks along the structure. $W' \le W$. The masks are used for trimming the coupling (Q_{RF}-factor).

Mostly calculations for this type of structure done with of GdfidL code [14]. There were investigated different shapes of cell and transit slit between the cells. The following numbers give an idea of parameters value. Typical longitudinal and transverse wakes *normalized to one cell* are $W_{\parallel} \cong -7\,kV/pC$ and $W_{\perp} \cong 2.2 \cdot 10^2\,V/pC/mm$ correspondingly for the accelerating structure with $l \cong 10mm$, $d = 2mm$, $W = 7mm$ (see Fig. 5) and the bunch with the longitudinal length $s_l \cong 1mm$ and bunch population $N \cong 10^6$. So total charge is $eN \cong 1.6 \cdot 10^{-13} C$ or $0.16pC$. An example of wake calculated is represented in Fig. 6. The charge in the bunch here is 0.2 *pC*. One can see, that the wake is slightly inductive. On Fig. 7 there is represented an example of wakes in a structure, obtained with GdfidL code.

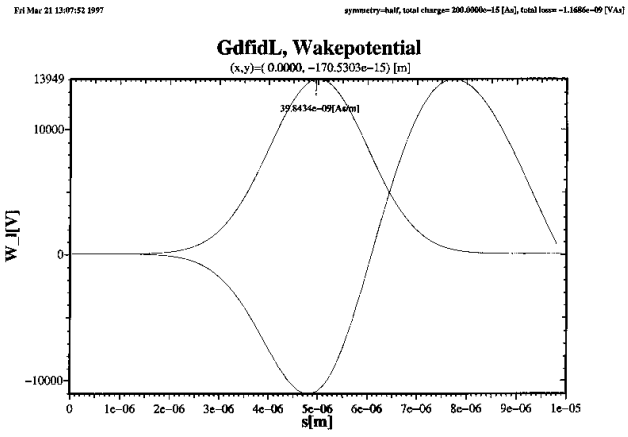

FIGURE 6. Example of the wake for 5 cells, Fig.7. Wake in the center of the bunch is about -10 *kV*.

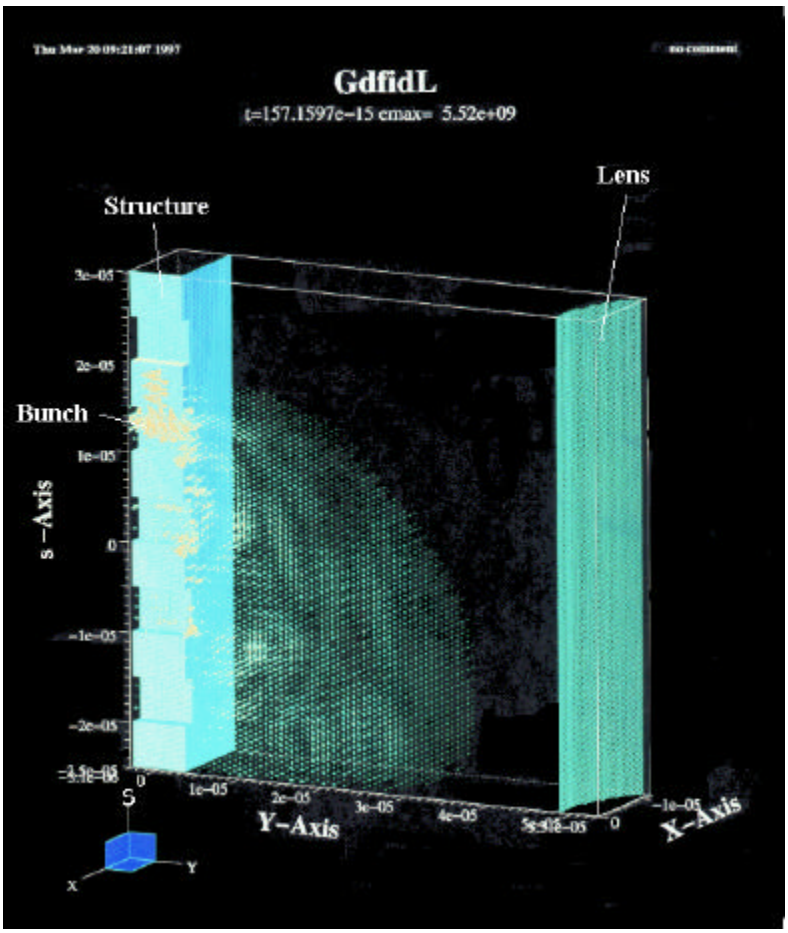

FIGURE 7. The bunch in the structure. A half of full picture is represented. The bunch is running through the structure on the left. A cylindrical lens (pos. 13 in Fig.3 is on the right side of the picture; ¼ is shown).

5. DEFLECTING DEVICE

The ratio of deflection angle J to diffraction angle $J_d \cong l/a$, where a is an aperture of the deflecting device, defines the *number of resolved spots (pixels)*, $N_R = J/J_d$. The deflection angle could be increased by some optics, but the number of resolved spots N_R is *an invariant* under any transformations. As we mentioned above, N_R value gives the number for the lowering the laser power for gradient desired and, also, the number for the duty time reduction. The last is important for the structure heating reduction. So it is desirable to have this number as big as possible.

Electro-optical devices use controllable dependence of refractive index on electrical field strength and direction applied to some crystals [5-10]. The change of reflecting index is equal to $Dn_i \cong (\P n_i / \P E_j) E^j(t)$. The refractive index in active media has a dependence like

$$1/n_i^2 = 1/n_{0i}^2 + \sum_j r_{ij} \cdot E^j , \qquad (2)$$

where r_{ij} –are 6×3 tensor[4]. This yields $\P n_i / \P E_j = -n_{0i}^3 r_{ij} / 2$ and the net change of refractive index becomes $Dn_i \cong (\P n_i / \P E_j) E^j(t) \cong -n_{0j}^3 r_{ij} E^j / 2$ (3)

For *ZnTe* (transparent for CO_2 radiation) having $n_0 \cong 2.9$, $r_{41} \cong 4.4 \cdot 10^{-12} m/V$ what gives for 10 *kV/cm* the refraction index change as much as $Dn \cong 10^{-4}$. For *KTN* (*Potassium Tantalate Niobate*) $Dn \cong 7 \cdot 10^{-3}$ for $l \cong 0.63 mm$ is possible [8].

To increase the N_R, a *multiple-prism* deflectors were developed, see Fig.8. Here neighboring prismatic crystals have reversed optical axes. These crystals positioned between strip–line electrodes. To be able to deflect short light bunches, the voltage pulse *V*(*t*) is propagating along this strip-line as a *traveling wave* together with the light to be deflected, as it was proposed in [1c]. This gives a necessary voltage profile along the light pulse at *cm* distances, what corresponds to the pulse duration $c\tau$. The wavefronts curvature radiuses in the deflected beam have a common center in the deflecting device. Necessary correction of this effect could be easily done, for example, by the thickness variation in cylindrical lens 14 in Fig.4. This variation is of the order of $\pm 80 mm$ [1c].

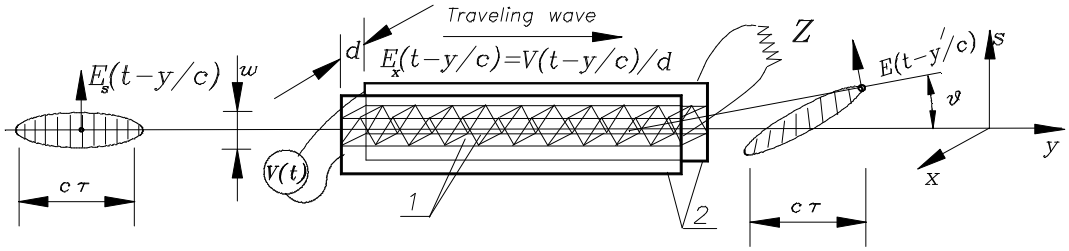

FIGURE 8. Prisms 1 with *oppositely directed optical axes* installed in series between two parallel strip–line electrodes 2, *d*–is the distance between them. *Z*– is a matching impedance. Lines across the laser bunch schematically show the wave fronts. $E_x(t - y/c)$–is a driving electrical field.

The deflection angle and the number of resolved spots become now

$$|DJ| \cong Dn \frac{2L_d}{w} \cong \frac{L_d}{w \cdot d} n_0^3 \cdot r_{ij} \cdot V, \qquad N_R \cong \Delta n \frac{2L_d}{l} \tag{4}$$

Where L_d stands for full length of deflecting device, *w*–is the light beam width (along direction of deflection). For *L*=50*cm*, one can expect for $w \cong 1cm$, that deflection angle is $\Delta J \cong 10^{-2}$ and $N_R \cong 10$ for $l \cong 10mm$ and, correspondingly $DJ \cong 10^{-2}$ and $N_R \cong 100$ for $l \cong 1mm$. We estimated the field applied to the crystals as 10 *kV/cm*. This is really a field strength *variation* along the light beam. This *variation is traveling with the light beam* along the deflecting device, Fig. 8. This strip-line deflecting device could be sectioned in terms of slicing for voltage reduction. For example, utilization of hundred slices in direction orthogonal to $w \cong 1$ *cm* will reduce the voltage to 0.1 *kV* per slice. If we suggest that electrical impedance of the strip-line is of the order $Z \cong 100 W$, the impulse power required to generate this voltage becomes $P \cong 100 W$ per slice, while

[4] Index *i* runs from 1 to 6. 1 stands for *xx*, 2–for *yy*, 3– *ss*, 4– for *ys*, 5–for *xs*, 6– for *xy*, *s*-longitudinal coordinate, see Appendix 2.

average one remains on the level $P_{av} \cong P \cdot f \cdot t \cong 16\ mW$ for repetition rate $f \cong 160\ Hz$. Special devices with avalanche diodes could be used here. The thickness of the package is defined by the level of the damage to the material of electro–optical crystal. We will see, that the laser flash energy passing through the single crystal is $10mJ$. In our example we estimated area as $S \cong w \cdot d$, what is about $1cm^2$. This yields the energy density 10 mJ/cm^2 only. One can decrease the area at least 10 (up to 100) times. Reduction of *w*, as one can see from (3) increases the deflection angle. Reduction of orthogonal dimension will further reduce the power required for deflection. Some optimization is possible here. Techical realization of this traveling wave deflector is represented in Fig. 9 below

cavities in a straight section. The straight sections narrowing at a center, so that they are geometrically congruent. Back and forward trajectories may be congruent also. The bends can be made to give a small input into cooling process. This yields the equilibrium emittances as for horizontal and vertical coordinate as the following[5] [2]

$$(\gamma\varepsilon_x) \cong 1\cdot 10^{-8}\ cm\cdot rad\ , \quad (\gamma\varepsilon_y) \cong 4\cdot 10^{-10}\ cm\cdot rad\ . \tag{5}$$

Scrapping extra particles remains a valid procedure for the emittance lowering on expense of particle population [1b]. Optical Stochastic Cooling [17] could be implemented here. Intra-Beam Scattering remains the general problem.

7. TRANSVERSE FOCUSING OF PARTICLE'S BEAM

A short wavelength of betatron oscillations helps against the resistive wall instability and wakefield influence reduction. The focusing system includes the quadrupole lenses of appropriate dimensions and a RF focusing [4]. Quadrupole lenses could be placed between the accelerating sections, see Fig.2, 6, 7. This type of focusing was considered in [1c]. *Focusing with quadrupole lenses only is acceptable for the accelerating structure scaled to a laser wavelength* $\lambda \cong 10\,mm$.

RF focusing occurs if the particle is going out of the RF crest [18]. If $x, y \neq 0$ the focusing parameters k could reach for $\lambda = 10\,mm$, $\gamma = 2\times 10^4$ (pc = 10 GeV), $W \approx 5mm$, $E_m \neq 10^{11} V/m$, $k_x \approx 2\cdot 10^5 \cdot Sin\varphi\ [m^{-2}]$. There are proposals to use this force for alternating phase focusing (APF), when the phase of the beam with respect to the RF crest is periodically changed, $\varphi = \pm\varphi_0$ [19]. In our case this can be made by arranging periodical delay of the accelerating light arriving to the grating, for example, by modulation of the thickness of the lens 13 in Fig. 3.

8. ACCELERATING GRADIENT

Let us suggest that full energy carried by a laser bunch is Q. For a time duration τ (see Fig. 2), we conclude, that the number n of periods in the bunch is about $n = \tau / T = c\tau / \lambda$, where $T = \lambda / c$ is period of radiation. So, the field energy stored in the volume corresponding to a half of period is $W_E \cong Q/2n$. From the other hand $W_E \cong (1/2)\varepsilon_0 E_m^2 V_{eff}$, where ε_0 is the dielectric permeability of the vacuum, $V_{eff} \cong gWh \cong g\lambda^2$ (W from Fig.8) is the effective volume, where the energy is concentrated. From the expressions for W_E, one can obtain the maximal field strength

$$E_m \cong \sqrt{Q/(\varepsilon_0 c\tau\ \lambda g)} \tag{6}$$

For estimation let us take $Q = 0.01J$, $\tau \cong 0.1\ ns$, $\lambda @ 1mm$, $g \cong \lambda/2 = 0.5mm$. This gives the field strength $E_m \cong 270\,GeV/m$. This value must be reduced by the factor, taking into account the longitudinal length l_f instead of g, see Fig.1. The longitudinal length could be

[5] With the wiggler's field oriented *vertically* and bending arcs in *horizontal* plane, the coordinates indicated here connected with the ones from Figs. 5, 7, 8 as $x \to y$; $y \to x$. This gives the minimum size of the beam for passing through the narrowings in the structure, marked with dimension d in Fig. 5 if it is installed as in Fig. 3,4.

estimated as a $l_f \approx L / N_R$, where L is the length of the structure. For $l @ 1mm$ one can expect $N_R \approx 100$, so the length of our interest is $l_f \approx ct / N_R$

For pumping the driving lasers the *diode laser arrays* could be used for the wavelengths indicated.

9. BUNCH POPULATION

The energy, accepted from the field by N particles is $W_a \cong eNE_m gI(g)$ where e is the charge of a particle, $I(g)$ is a function of the order of unity – an analog of the transit time factor. The share of the energy will be

$$hW \cong h\frac{1}{2}Q\,l/(ct) \cong eNgI(g)\sqrt{Q/\left(e_0 ct\ \ l\ g\right)} \qquad (7)$$

(7) yields

$$N \cong \frac{h}{2eI(g)}\sqrt{\frac{e_0 l^3 Q}{ct\ g}}. \qquad (8)$$

With $I(g)$= 0.5, $h \approx 0.05$ (5%), this gives N @ $1\cdot 10^6$ for $l \cong 1mm$. For $l \cong 10mm$ this number will be $N \cong 3\cdot 10^7$.

10. FINAL FOCUS

We suggested to arrange a final focusing for our purposes with *a multiplet* of FODO structures having the number of the RF lenses in it of the order of few hundreds [1b]. The gradient in these lenses must vary from the very strong at the side closest to IP, to the weak one at the opposite side of the multiplet. Focusing properties of these RF lenses, discussed above can be used here. A laser radiation of general and *multiple* frequency can be used for such focusing. This is so called Adiabatic Final Focus. *Such a tiny lens, not sensitive to detector magnetic field could be easily installed inside the detector*.

11. LUMINOSITY

For luminosity we have the formula

$$L \cong \frac{N^2 f H_B g\ N_B}{4p\sqrt{(ge_x)(ge_y)}\cdot b_x b_y}\ , \qquad (9)$$

where H_B is the enhancement parameter, N_B – is the number of bunches per train. For emittances from (2, 3) one can obtain L here for $b_x \approx b_y \approx 0.3\,l$, $l \cong 10mm$, g= 2×10^6 (pc=1TeV), $N \cong 2\cdot 10^7$, $f \cong 160Hz$, $H_B \cong 2$, N_B=1 as $L \approx 1\cdot 10^{33} cm^{-2}s^{-1}$. For $l \cong 1mm$ result will be about the same as the number of the particles is lower here. The transverse dimensions will be $s_x \cong 1.2\cdot 10^{-9}\ cm \equiv 0.12\ \mathring{A}$, $s_y \cong 1.4\cdot 10^{-10}\ cm \equiv 0.024\ \mathring{A}$. Effective longitudinal distance between the particles has the order $l_b / N \approx l / N$. The last number in our case is formally $\le 10^{-11} cm$. As the distance $\approx D_C \cong 3.8\cdot 10^{-11} cm$ is absolute limit for such a spacing, we conclude that in each transverse slice $\approx D_C$ the number of the particles $\approx 1-2$. The dimension as above, formally corresponds to ≈ 4 particles per slice. As in each transverse slice $\approx D_C$ the number of the particles $\approx 1-2$. As we mention in previous section 12, the transverse dimensions formally correspond to ≈ 4 particles per slice. So the radiation is going in very strong quantum regime and models with coherent

field are not applicable here. Strong reduction of radiation one can expect due to Landau-Pomeranchuk effect [22]. The radiation processes required more detailed considerations, however. *Using a train of bunches* (up to 100, see above) one can decrease the number of the particles in each bunch and/or to increase the cross section of the beam, thereby allow some reasonable losses. A small *crossing angle* required to prevent illumination the final lenses by used beam. This angle is absolutely necessary for multi- bunch operational mode. Tiny dimensions of the beam can help to push the beams through.
The possibility of operation with high repetition rate, up to *few kHz* is open.

12. CONCLUSION

Any point of accelerating structure must be illuminated for the minimal time in order to avoid the damage associated with the overheating. Greater accelerating gradient requires higher power density of radiation at the structure. *Traveling Laser Focus*, *TLF*- method solves both problems. Illuminating time and total laser power (or the flash energy) both defined by the number of resolved spots (pixels) associated with a deflecting device. The *traveling wave* regime is required for this device. Number of resolved spots $\approx 20-100$ achievable. The necessity to obtain the beta function at Interaction Point (IP) region below $1\,mm$ requires very strong focusing, what can be arranged with RF lenses. The electromagnetic collisions at IP are going in deep quantum regime and require additional considerations. A multi-bunch regime can diminish the problems associated with radiation. Repetition rate is another extensive parameter for further increase of luminosity with rejected bunch population. Here a factor of ten is visible.
Polarization of colliding beams could be a crucial issue in reduction of electromagnetic background at IP.
Lasers for the TLF method need to have more power in intermediate time duration $t \approx 100\,ps$ rather than in a shorter time interval. Equivalent time of illumination of accelerating structure with this pulse is $0.1 \div 1\,ps$, however.
For a $0.5\times 0.5\,TeV$ Collider the length becomes $2\times 170\ m$ for $l \cong 10\,mm$ and $2\times 17\ m$ for $l \cong 1\,mm$ correspondingly. One can compare these numbers with that from Linear Collider projects in consideration in many Laboratories around the World ($2\times 10\ km$ gives about $2\times 500\ GeV$)
In conclusion we can say, that TLF method what brings a Laser driven Linac to a present day front technology, could be considered as a challenge for LLC.

13. REFERENCES

[1] A.A. Mikhailichenko, a) "The method of acceleration of charged particles", Author's certificate USSR N 1609423, Priority May 1989, Bulletin of Inventions (in Russian), N6, p.220, 1994. b) "A concept of a Linac Driven by a Traveling Laser Focus", 7th Advanced Accelerator Concepts Workshop, AIP 398 Proceedings, p.547. c) "Laser Acceleration: a Practical Approach", CLNS 97/1529, Cornell, 1997; also a Talk on LASERS'97, Fairmont Hotel, New Orleans LA, December 15-19, 1997.

[2] A.A. Mikhailichenko, "Injector for a Laser Linear Collider", this Workshop.

[3] A.A. Mikhailichenko, "On the physical limitations to the Lowest Emittance ", Ref. [1b], p.294 and CLNS 96/1436, Cornell, 1996 .

[4] A.A. Mikhailichenko, "A Beam Focusing System for a Linac Driven by a Traveling Laser Focus", PAC97, Dallas, TX, Proceedings, p.784.

[5] C.L. Ireland, J.M. Ley, "Electrooptical Scanners" in "Optical scanning", Edited by G. Marshall, Marcel Dekker, Inc., 1991.

[6] *Selected Papers on Laser Scanning and Recording*, *SPIE* Vol. 378, Editor L. Beiser, 1985.

[7] V.J.Fowler, J.Schlafer, *Applied Optics*, Vol.5, N10, 1657(1966)

[8] F.S.Chen et. al., Journ. *Applied Physics*, Vol.37, N1, p.388(1966).

[9] J.F. Lotspeich, *IEEE Spectrum*, 45 (Feb. 1968), see also [5].

[10] L. Bademain, "Acousto-Optical Laser Recording" in [6], p.255.

[11] J. Rosenzweig, A. Murokh, C. Pellegrini, *Phys. Rev. Let*. **74**, 2467(1995).

[12] R.C.Fernow, J.Claus, AIP Conference Proceedings, 279, 1992, p.212.

[13] H.Henke,"mm Wave Linac and Wiggler structure", EPAC 94, London.

[14] W. Bruns, **GdfidL,** TU Berlin, 1997.

[15] C.Kittel, *Introduction to Solid State Physics*, Wiley, NY, 1976.

[17] A.A. Mikhailichenko, M.S.Zolotorev, "Optical Stochastic Cooling", *Phys. Rev. Let*. **71**, 4146(1993).

[18] W. Schnell, "Microwave quadrupoles for linear colliders", CLIC Note 34, 1987.

[19] F.E.Mills, A. Nassiri, Argonne National Laboratory, internal report ANL/APS/MMW-9, 1994.

[20] V.N.Baier, V.M. Katkov, BINP 97-70, Novosibirsk 1997.

[21] A.A. Mikhailichenko, SLAC-R-502, p.229.

[22] Ch. C. Davis, *Lasers and Electro-Optics. Fundamentals and Engineering*, Cambridge, 1996.

APPENDIX 1.

Here we demonstrate schematically a

Theorem:

If electromagnetic field of some configuration accelerates particles, it has the electrical field maximal value on the surrounding boundaries.

Demonstration.

Without any restriction to the common case, let us consider *TEM* field. This type defined by equations

$$\vec{\nabla}\times\vec{E}\big|_S=\frac{\partial E_y}{\partial x}-\frac{\partial E_x}{\partial y}=-\frac{\partial B_s}{\partial t}=0 \tag{A1.1}$$

The components of electromagnetic field could be represented as the following

$$\overline{E}=E_x-iE_y=\frac{\partial W}{\partial z}+\frac{\partial W}{\partial \overline{z}},\quad E_S=\int\left(\frac{\partial^2}{\partial s^2}-\frac{1}{c^2}\frac{\partial^2}{\partial t^2}\right)W(z,\overline{z},s,t)ds$$

$$B_S\equiv 0,\qquad \overline{B}=B_x-B_y=ie_0\frac{\partial}{\partial t}\int\overline{E}(z,\overline{z},s,t)ds, \tag{A1.2}$$

where $z=x+iy$, $\overline{z}=x-iy$, $i^2\equiv -1$, s - is a longitudinal coordinate,

$$\frac{\partial}{\partial z}\equiv\frac{1}{2}\left(\frac{\partial}{\partial x}-i\frac{\partial}{\partial y}\right),\quad \frac{\partial}{\partial \overline{z}}\equiv\frac{1}{2}\left(\frac{\partial}{\partial x}+i\frac{\partial}{\partial y}\right). \tag{A1.3}$$

With definition (A1.3) Laplasian could be expressed as the following

$$\nabla^2\equiv\frac{\partial^2}{\partial x^2}+\frac{\partial^2}{\partial y^2}+\frac{\partial^2}{\partial s^2}=4\frac{\partial^2}{\partial z\,\partial\overline{z}}+\frac{\partial^2}{\partial s^2}. \tag{A1.4}$$

Complex potential $W(x,y,s,t)\equiv W(z,\overline{z},s,t)$ satisfies the equation

$$4\frac{\partial^2 W}{\partial z\,\partial\overline{z}}+\left(\frac{\partial^2}{\partial s^2}-\frac{1}{c^2}\frac{\partial^2}{\partial t^2}\right)W(z,\overline{z},s,t)=0. \tag{A1.5}$$

Electromagnetic field accelerates the particle if it provides the energy change

$$DE = \int_{-\infty}^{+\infty} (\vec{F} \cdot \vec{v}) dt = e \int_{-\infty}^{+\infty} (E_S \cdot v) dt \cong ec \int_{-\infty}^{+\infty} E_S dt \Big|_{s=ct}, \quad \text{(A1.6)}$$

where $(\vec{F} \cdot \vec{v})$ –is an instant power, *F*–is the force. Integrals are taken along the trajectory of the (relativistic) particle. Let us introduce the complex potential *U*, so that $W(z,\bar{z},s,t) = \partial U / \partial s$. One can see, that this is basically a *s*-component of Hertz's vector. This potential satisfies the same equation (A1.5) and introduced here for simplification of expressions. With this potential longitudinal component of electrical field becomes

$$E_S = \left(\frac{\partial^2}{\partial s^2} - \frac{1}{c^2} \frac{\partial^2}{\partial t^2} \right) U(z,\bar{z},s,t) = -4 \frac{\partial^2 U}{\partial z \partial \bar{z}}. \quad \text{(A1.7)}$$

From last expression one can see, that any plane electromagnetic wave in *s*-direction ($U = U(s-ct)$) does not have longitudinal components, and, hence, does not accelerate particles moving along straight line. One can see from here, that the source of longitudinal component associated with nonzero derivative $\partial / \partial \bar{z} \neq 0$. This nonzero derivative in it's turn associated with nonzero longitudinal derivative, i.e. potential must vary in longitudinal direction. A condition (A1.6) that the field of some particular configuration *accelerates* particles could be expressed now as the following

$$c \int_{-\infty}^{+\infty} E_S dt = \int \left(\frac{\partial^2}{\partial s^2} - \frac{1}{c^2} \frac{\partial^2}{\partial t^2} \right) U(z,\bar{z},s,\frac{s}{c}) ds = 4 \frac{\partial^2}{\partial z \partial \bar{z}} \int U(z,\bar{z},s,\frac{s}{c}) ds \neq 0. \quad \text{(A1.8)}$$

One can see from last expression, that for nonzero acceleration condition the potential derivation $\partial U / \partial \bar{z} \neq 0$. This means, formally, that the potential as a function of complex variable is an analytical function[6] only at the axis, $|z| = 0$. This function provides a *quasiconformal* transformation[7].

Solution for *U* could be represented as the following

$$U(z,\bar{z},s,t) = \sum_{m=-\infty}^{\infty} \sum_{k=0}^{\infty} E_{m-1,k}(s,t) \cdot z^{m+k} \cdot \bar{z}^k, \quad \text{(A1.9)}$$

where functions $E_{m-1,k}$ satisfy the recurrent formula

$$E_{m-1,k}(s,t) = \frac{(-1)^k}{4^k k!(m+k)\cdots(m+1)} \cdot \left(\frac{\partial^2}{\partial s^2} - \frac{1}{c^2} \frac{\partial^2}{\partial t^2} \right)^k E_{m-1,0}(s,t). \quad \text{(A1.10)}$$

Functions $E_{m-1,0}(s,t)$ define the multipole contents for any particular configuration.

Now expression (A1.7) could be represented as the following

$$E_s(z,\bar{z},s,t) = \sum_{m=-\infty}^{\infty} z^m \sum_{k=0}^{\infty} \frac{(-1)^k \cdot |z|^{2k}}{4^k k!(m+k)\cdots(m+1)} \cdot \left(\frac{\partial^2}{\partial s^2} - \frac{1}{c^2} \frac{\partial^2}{\partial t^2} \right)^{k+1} E_{m-1,0}(s,t), \quad \text{(A1.11)}$$

or

$$E_s(z,\bar{z},s,t) = 4 \sum_m z^m \sum_k E_{m-1,k}(s,t) \cdot (m+k) \cdot k \cdot |z|^{k-1}$$

$$\bar{E} = E_x - iE_y = \frac{\partial^2 U}{\partial z \partial s} + \frac{\partial^2 U}{\partial \bar{z} \partial s} = \sum_{m=0}^{\infty} z^{m-1} \sum_{k=0}^{\infty} \frac{\partial E_{m-1,k}(s,t)}{\partial s} \cdot |z|^{2k-2} [(m+k) \cdot |z|^2 + k \cdot z^2]$$

According to (A1.8) $$\int \left(\frac{\partial^2}{\partial s^2} - \frac{1}{c^2} \frac{\partial^2}{\partial t^2} \right)^{k+1} E_{m-1,0}(z,\bar{z},s,\frac{s}{c}) ds = Const \neq 0, \quad \text{(A1.12)}$$

---

[6] Function $U(z, \bar{z})$ is analytical if $\partial U / \partial \bar{z} = 0$ - the Cauchi-Rieman condition.

[7] Physical sense for this is clear. In 3-D case some lines escape from a single plane of complex *z* to other associated planes in *s*-direction proportionally to derivative in this direction. Namely this deficit, associated with changing the picture in longitudinal direction from mathematical point of view yields nonalytical behavior in complex plane for any particular (fixed) value *s*.

Now one can see, that function, described by (A1.9) reaches it's minimum on the axis, $|z| = 0$, and, hence,

the maximum value $|E|^2 = E_x^2 + E_y^2 + E_s^2 = |E|^2 + E_s^2$ reaches at the boundaries, surrounding the acceleration region. **Q.E.D.**

APPENDIX 2

Indicatrix allows to determinate the refraction index *n* components for monochromatic plane waves as a function of their polarization. For Cartesian coordinate system with the principal axes of a crystal, the indicatrix can be represented as

$$\left(\frac{1}{n^2}\right)_1 x^2 + \left(\frac{1}{n^2}\right)_2 y^2 + \left(\frac{1}{n^2}\right)_3 s^2 + 2\cdot\left(\frac{1}{n^2}\right)_4 ys + 2\cdot\left(\frac{1}{n^2}\right)_5 xs + 2\cdot\left(\frac{1}{n^2}\right)_6 xy = 1\cdot \qquad \text{(A2.1)}$$

For electro-optic effect, an electric field applied, changes each of coefficients in (A2.1) so that they linearly dependent on electrical field applied as (2). With abbreviation $D(1/n)_i = 1/n_i - 1/n_{0i}$ this could be rewritten as the following

$$\begin{pmatrix} D(1/n^2)_1 \\ D(1/n^2)_2 \\ D(1/n^2)_3 \\ D(1/n^2)_4 \\ D(1/n^2)_5 \\ D(1/n^2)_6 \end{pmatrix} = \begin{pmatrix} r_{11} & r_{12} & r_{13} \\ r_{21} & r_{22} & r_{23} \\ r_{31} & r_{32} & r_{33} \\ r_{41} & r_{42} & r_{43} \\ r_{51} & r_{52} & r_{53} \\ r_{61} & r_{62} & r_{63} \end{pmatrix} \times \begin{pmatrix} E_x \\ E_y \\ E_s \end{pmatrix}, \qquad \text{(A2.2)}$$

where vector $\vec{E} = \{E_x, E_y, E_s\}$ describes the electrical driving field applied. So if original axes are the principal ones, the indicatrix becomes [22]

$$\left[\frac{1}{n_x^2} + D\left(\frac{1}{n^2}\right)_1\right]x^2 + \left[\frac{1}{n_y^2} + D\left(\frac{1}{n^2}\right)_2\right]y^2 + \left[\frac{1}{n_s^2} + D\left(\frac{1}{n^2}\right)_3\right]s^2 + 2\cdot D\left(\frac{1}{n^2}\right)_4 ys + 2\cdot D\left(\frac{1}{n^2}\right)_5 xs + 2\cdot D\left(\frac{1}{n^2}\right)_6 xy = 1\cdot \qquad \text{(A2.1)}$$

For the parameters under discussion at the deflecting device, see Fig.6, the power density. $10mJ/(w\cdot d)^2 \cong 10mJ/cm^2$ with $t \cong 100$ *ps* duration, yields the laser electrical field strength of the order 1% of the driving electrical field. If any of components $r_{i3} = 0$, then laser field does not influence to the deflection at all.

As we mentioned above, typical values of the r_{ij} are of the order $\cong 10^{-12} m/V$. For example, for *GaAs (ZnSe, CdTe)* cubic structure and for *KDP (ADP, $CdGeAs_2$)* tetragonal structure we have correspondingly

$$(r)_{ij} = \begin{pmatrix} 0 & 0 & 0 \\ 0 & 0 & 0 \\ 0 & 0 & 0 \\ 1.5 & 0 & 0 \\ 0 & 1.5 & 0 \\ 0 & 0 & 1.5 \end{pmatrix} \times 10^{-12}[m/V], \qquad (r)_{ij} = \begin{pmatrix} 0 & 0 & 0 \\ 0 & 0 & 0 \\ 0 & 0 & 0 \\ 8.8 & 0 & 0 \\ 0 & 8.8 & 0 \\ 0 & 0 & 10.5 \end{pmatrix} \times 10^{-12}[m/V] \qquad \text{(A2.3)}$$

For example, with driving field applied in *x*-direction, E_x, (normal to direction of acceleration), the indicatrix according to (A2.2) becomes

$$\frac{x^2}{n_0^2} + \frac{y^2}{n_0^2} + \frac{s^2}{n_e^2} + 2\cdot r_{41}E_x \cdot ys \cong 1 \qquad \text{(A2.4)}$$

So one can see that the principal axes have a new directions. The new principal axes of ellipsoid (A2.4) has an angle $\cong r_{41}E_x / n_e^2$ to the previous one. Accelerating field has a component parallel to *s*, E_s^a. Component of accelerating field in *y* direction at out of deflection device is $E_y^a \cong E_s^a \cdot D\,J$. So the cut could be made so that the prisms have their orthogonal edges parallel to old principal axes.